Oxygen adsorption on the clean and O-precovered Fe (110) and (100) surfaces

2007 J. Phys.: Condens. Matter 19 096011

(http://iopscience.iop.org/0953-8984/19/9/096011)

IOP Publishing Journal of Physics: Condensed Matter

J. Phys.: Condens. Matter **19** (2007) 096011 (8pp) doi:10.1088/0953-8984/19/9/096011

Oxygen adsorption on the clean and O-precovered Fe (110) and (100) surfaces

P Błoński[1,2], **A Kiejna**[1] **and J Hafner**[2]

[1] Institute of Experimental Physics, University of Wrocław, Plac M. Borna 9, PL-50-204 Wrocław, Poland
[2] Institut für Materialphysik and Center for Computational Materials Science, Universität Wien, Sensengasse 8/12, A-1090 Wien, Austria

E-mail: kiejna@ifd.uni.wroc.pl

Received 5 December 2006, in final form 26 January 2007
Published 14 February 2007
Online at stacks.iop.org/JPhysCM/19/096011

Abstract

The chemisorption of atomic oxygen on clean and oxygen-precovered Fe(100) and Fe(110) surfaces has been studied using *ab initio* density-functional techniques. It is demonstrated that although on both surfaces the adsorption of oxygen atoms remains an unactivated process up to full monolayer coverage, important differences are to be expected on exposure to molecular oxygen. The reason is that while on Fe(100) the differential heat of adsorption is almost independent of the O-coverage, the differential heat of adsorption on Fe(110) decreases strongly with increasing coverage. For coverages of 0.5 ML O or higher, the energy gain by adsorbing an additional O atom is comparable or lower than the energy (per atom) required to dissociate an O_2 molecule. The consequences on the formation of thin-film oxides are discussed.

(Some figures in this article are in colour only in the electronic version)

1. Introduction

The interaction of oxygen with iron surfaces leading to dissociation and adsorption is a determining factor for processes such as oxidation, passivation, corrosion, and catalysis. The progress of unwanted corrosion of iron surfaces can be stopped or significantly slowed down through the formation of passive films. Oxidized metal surfaces play an important role in heterogeneous catalysis. Furthermore, Fe-oxides are also of potential technological significance because of the magnetic properties of these systems. An improved understanding of the mechanism of oxidation is thus fundamental to many important technological processes. For this reason, oxygen adsorption on Fe surfaces has been studied extensively, both experimentally [1–19] and theoretically [20–24]. The experimental studies have identified at least three distinct stages of oxygen adsorption on iron surfaces: (i) chemisorption of atomic oxygen or dissociative chemisorption of O_2 molecules at the surface, (ii) formation of thin-film oxides with incipient penetration of oxygen into deeper layers, and (iii) growth of bulk oxides. The assignment of experimental signatures in photoemission, Auger electron, and electron energy loss spectroscopies to structural models, based of density-functional calculations, was found to be very important for identifying the limit between adsorption and oxidation.

These investigations have also highlighted quite different scenarios for oxygen adsorption on the low-index surfaces of iron. On Fe(100) high-temperature adsorption leads to the formation of a $p(1 \times 1)$ surface structure, identified as full monolayer coverage of atomic oxygen, preceded by the formation of $p(2 \times 2)$ and $c(2 \times 2)$ superstructures at lower coverage. At low temperatures, the sticking probability S remains close to unity up to a coverage of $\Theta \sim 0.8$ ML, followed by a very sharp drop to almost zero sticking. Kinetics at room temperature shows a quite different behaviour: S decreases linearly up to about $\Theta \sim 0.5$ ML, followed by a plateau at $\Theta \sim 0.35$ ML up to $\Theta \sim 1$ ML and a further linear decrease [12–15]. The close-packed Fe(110) surface shows a much slower oxygen uptake; at high temperatures saturation occurs at $\Theta \sim 0.4$ ML, preceded by the formation of transitory $c(2 \times 2)$ and $c(3 \times 1)$ superstructures. The sticking probability decreases linearly up to saturation, followed by a maximum at higher oxygen exposure. The minimum in the sticking probability marks the onset of oxide film formation, first in the form of an FeO(111)/Fe(110) film, followed by the growth of an Fe_3O_4 film on-top of the FeO layer [1–7]. For the open Fe(111) surfaces, conflicting results are found in the literature. While Viefhaus and Grabke [1] report that the Fe(111) surface is unstable in equilibrium with a Fe–FeO mixture, Narkiewicz and Arabczyk [16], report a linear decrease of the sticking probability up to the formation of a $p(1 \times 1)$ O-adlayer.

In relation to the technological importance of the O/Fe surface system, *ab initio* density-functional studies of oxygen on Fe surfaces are comparatively scarce [20–24]. Moreover, most calculations consider only the energetics and the structural, electronic and magnetic properties of adsorbed O up to a full monolayer coverage. To the best of our knowledge, our previous work [24] on atomic oxygen at the Fe (110) and (100) surfaces represents the first attempt to extend density-functional studies beyond the O-monolayer limit and to investigate the incipient stages of oxide formation. On the Fe(100) surface, completion of a full monolayer of on-surface O is immediately followed by incorporation of additional oxygen atoms in subsurface octahedral positions, inducing a strong expansion of the interlayer distance. This makes the near surface structure of the O/Fe film fcc-like, in analogy to the rocksalt structure of FeO. On Fe(110) the experimental studies [7–9] reported the formation of well-defined, ordered oxygen overlayers only up to sub-monolayer O-coverage: $p(2 \times 2)$, $c(2 \times 2)$, and $c(3 \times 1)$ structures have been identified, followed by the growth of a thin-film iron oxide. This is supported by an experiment by Vescovo *et al* [10], according to which no $p(1 \times 1)$ oxygen overlayer is formed at 300 K. Our first-principles study of O/Fe(110) shows that under reductive conditions (up to the limiting value for the chemical potential of oxygen set by the difference in the free energies of bulk FeO and Fe), a $p(2 \times 2)$ O/Fe(110) phase is stable, but that coverages of $\Theta = 0.5$ ML or higher are unstable with respect to the formation of FeO, in agreement with experimental observation [11, 18, 19]. However, thin-film oxides with simple structures based on the incorporation of O in tetrahedral and/or octahedral subsurface sites of bcc Fe are energetically not competitive, except at very high partial pressures of oxygen. Admittedly, our calculations produced only the integral heats of adsorption for oxygen adlayers of a fixed composition—the influence of a precoverage by a sub-monolayer amount of oxygen on the energetics of chemisorption has not been considered. This is precisely the aim of the present work: we shall explore the potential energy surface of an oxygen atom approaching a Fe(100) or Fe(110) surface precovered with an increasing amount of oxygen.

2. Computational details

All calculations were carried out using the Vienna *ab initio* simulation package (VASP) [25] performing a variational solution of the Kohn–Sham equations of density functional theory (DFT) in a plane-wave basis. The spin-polarized version of the exchange–correlation functional proposed by Perdew and Wang (PW91) [26], based on the generalized gradient approximation (GGA) was used. It is important to emphasize that only the GGA approximation yields the correct structural and magnetic ground-state structure of bulk Fe [27, 28]. In order to allow comparison with our previous study of O adsorption on the Fe (110) and (100) surfaces [24], the electron–ion interactions are represented by ultrasoft pseudopotentials (USPP) [29, 30]. A plane-wave basis with energy cutoff of 400 eV was used to expand the electronic wavefunctions. Brillouin zone integrations were performed on a $4 \times 4 \times 1$ special k-point mesh (for the 2×2 surface unit cell) generated by the Monkhorst–Pack scheme [31]. To accelerate convergence, fractional occupancies of the eigenstates near the Fermi level with a first-order Methfessel–Paxton [32] smearing of 0.2 eV were adopted. The calculated lattice constant ($a_{\mathrm{th}} = 2.863$ Å) used in this study is in good agreement with experiment ($a_{\mathrm{exp}} = 2.867$ Å [33]).

The surfaces were modelled by slabs consisting of five Fe layers separated by a vacuum layer of $\simeq 20$ Å and repeated periodically. This slab thickness has been shown [34] to be sufficient to represent well a semi-infinite iron crystal and its compact surfaces. Adsorbate atoms were placed on one side of the slab and a dipole correction [35, 36] was applied to compensate for an artificial electric field arising from the asymmetry of the slab. The positions of Fe atoms in the two topmost layers, and of all O atoms, were optimized until the forces on all unconstrained atoms converged to less than 0.02 eV Å^{-1}. The distance of the adsorbing oxygen atom from the surface was gradually decreased for a series of intermediate states distributed along the reaction path connecting the initial and final states via the nudged elastic band method [37].

3. Results and discussion

The potential energy of an O-atom approaching the clean and oxygen precovered (110) and (100) iron surfaces was calculated as the total energy difference with respect to the energy of an isolated oxygen atom, E^{O} and the energy E^{X} of the surface (clean or precovered) before adsorption,

$$E = E^{\mathrm{O/X}} - E^{\mathrm{X}} - E^{\mathrm{O}}. \tag{1}$$

Here, $E^{\mathrm{O/X}}$ is the total energy of the slab plus the adsorbing O atom. The potential-energy difference defined by equation (1) measures the *differential* heat of adsorption of O on a precovered surface. The O coverage Θ is defined as the ratio of the number of adsorbed oxygens to the number of atoms in an ideal substrate layer.

3.1. Clean and O precovered Fe(100)

Previous theoretical studies [21, 23, 24] have identified the fourfold hollow (fh) as the stable adsorption site for oxygen on Fe(100). Therefore we have calculated the potential energy profiles for an O-atom located vertically above a vacant fh site, approaching the clean and O-precovered surface, and finally adsorbing in the fh position.

The potential energy curves (figure 1) show no barrier to adsorption, independent of the precoverage. Adsorption of O in the fh sites of the clean surface is a non-activated process. At

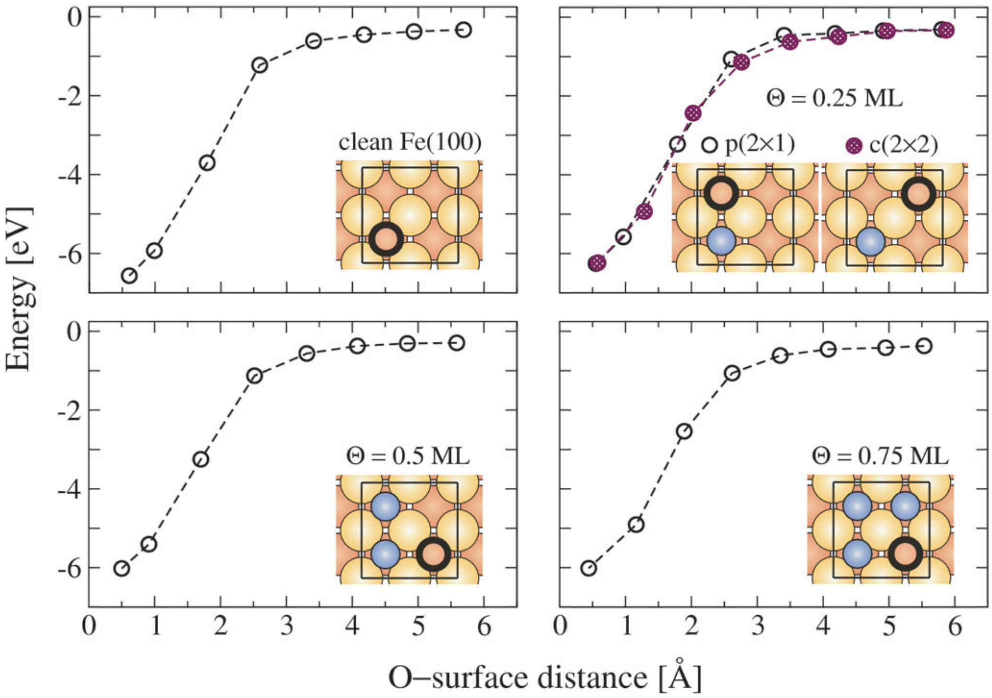

Figure 1. Potential energy profiles for O adsorption on the clean and O-precovered Fe(100) surfaces. Insets display the initial and final configurations: filled circles represent preadsorbed oxygen, open circles—O atom approaching the surface.

an O-precoverage of 0.25 ML, two different configurations were explored. With the additional O atom in its final position, either a $p(2 \times 1)$ or a $c(2 \times 2)$ structure is formed. The results presented in figure 1 show that the differential heat of adsorption, i.e. the energy gain of the O atom on binding to the O-precovered surface, is only weakly dependent on the O pre-coverage. The differential adsorption energy of an oxygen adsorbing on an O/Fe(100) surface precovered with 0.75 ML of oxygen and completing a $p(1 \times 1)$ monolayer is only 17% lower than the adsorption energy on a clean Fe(100) surface. The strong O–Fe binding is also reflected in the structure of the adlayer: with increasing coverage, the height of the adsorbed O above the surface decreases by about 26%, from 0.61 Å at 0.25 ML to 0.45 Å at a full 1 ML coverage (experiment: 0.53 ± 0.06 Å [20]). Oxygen adsorption also modifies the interlayer distance in the substrate; while on a clean Fe(100), the first interlayer distance contracts by -3%, on O-covered surface an outward relaxation increasing from 2% at a coverage of 0.25 ML to 16% at full monolayer coverage is predicted. This shows that, as in other thin-film oxides [38, 39], the distance between the oxide layer and the substrate increases, reflecting a reduced interaction strength.

The *integrated* adsorption energy, $E_{\rm ad}$, calculated with respect to the energy per O-atom in an O_2 molecule according to

$$E_{\rm ad} = \frac{1}{N}\left(E^{\rm O/Fe} - E^{\rm Fe} - \frac{1}{2}E^{\rm O_2}\right), \tag{2}$$

(where N is the number of oxygen atoms in the unit cell, $E^{\rm O/Fe}$ is the total energy of the O-covered Fe slab, $E^{\rm Fe}$ is the total energy of the clean Fe substrate, and $E^{\rm O_2}$ is the energy of a free

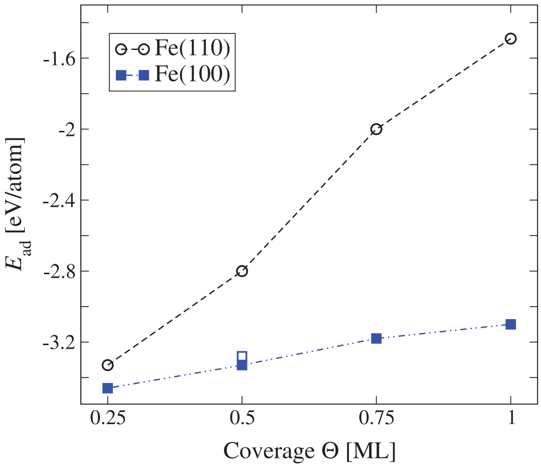

Figure 2. Integrated adsorption energy per adatom, E_{ad}, calculated according to equation (2) as a function of coverage of O on Fe (110) and (100). The empty square marks the value for O adsorbed on Fe(100) in the $c(2 \times 2)$ structure.

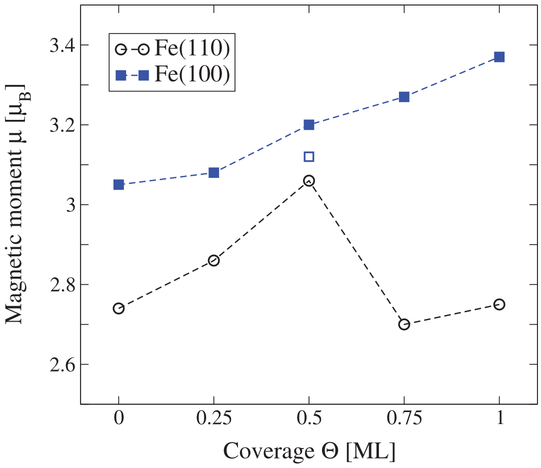

Figure 3. The local magnetic moments μ of Fe-atoms in the topmost layer of O/Fe(100) and O/Fe(110), plotted as a function of O-coverage. The empty square marks the value for O adsorbed on Fe(100) in the $c(2 \times 2)$ structure.

O_2 molecule) decreases only slightly with increasing coverage. For $\Theta = 1$ ML the adsorption energy is only by about 10% smaller than at 0.25 ML, it scales linearly with the O-coverage (figure 2).

As already mentioned, the structure of a full monolayer of O/Fe(100) resembles an ultrathin oxide film with the rocksalt structure of FeO (wustite) [24]. The O–Fe bond length of 2.07 Å corresponds closely to the value of 2.15 Å in bulk FeO (the difference does not exceed 4%). Also, at the completely covered Fe(100) surface, the local magnetic moment of 3.37 μ_B of Fe atoms in the topmost layer has a value comparable to the local moment in bulk FeO (3.32 μ_B [40]). Quite generally the presence of on-surface oxygen enhances the magnetism at the surface (see figure 3). The calculated local magnetic moments on the Fe-atoms in the surface layer increase linearly (from 3.05 μ_B at the clean surface) with the O-coverage.

The formation of a $p(1 \times 1)$ overlayer structure has also been observed experimentally [14, 20, 41], and has been ascribed there to incipient formation of an ultrathin FeO film. For further details of the electronic structure of O/Fe(100) films we refer to our previous work [24].

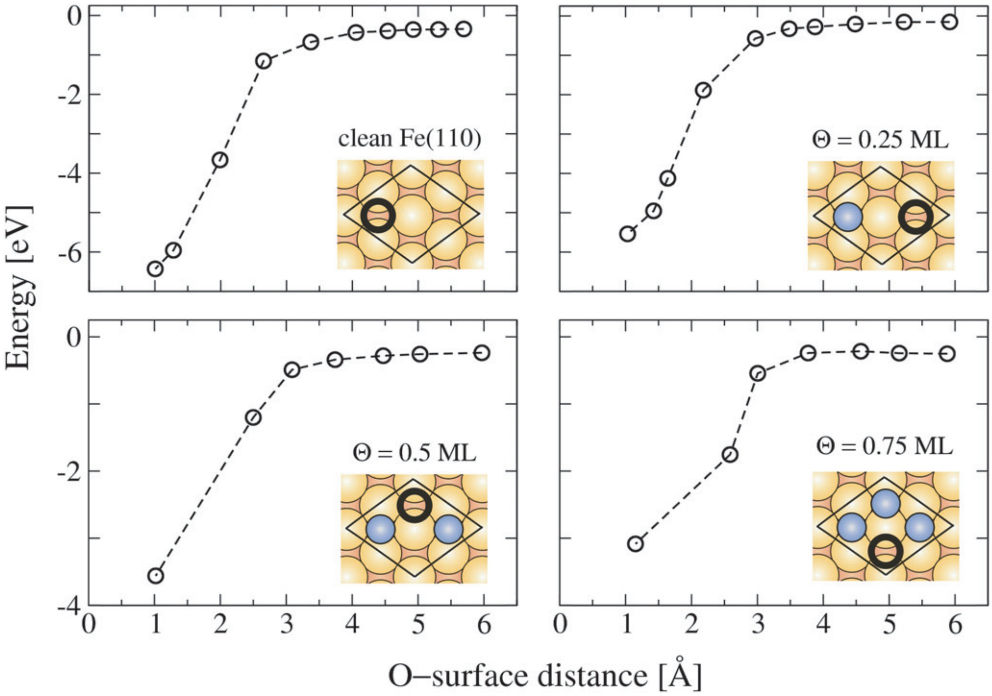

Figure 4. Potential energy profiles for O adsorption on clean and O-precovered Fe(110) surfaces. Insets display the initial and final configurations: filled circles represent preadsorbed oxygen, open circle—O atom approaching the surface.

3.2. Clean and O precovered Fe(110)

We now turn to oxygen adsorption on the clean and O-precovered (110) surface of iron. We have computed the one-dimensional potential energy profiles for an oxygen atom approaching a clean surface and surfaces precovered with 0.25, 0.5 and 0.75 ML of oxygen, respectively. The final adsorption structures for $1/4$ and $1/2$ ML correspond to $p(2\times2)$ and $c(2\times2)$ periodicities, respectively. Since previous calculations [23, 24] have identified the two-fold long bridge (lb) site as the stable adsorption position, in agreement with experiments [7, 42], the approaching O atom was put directly above the lb position (see insets in figure 4). Surprisingly, figure 4 shows that there is no barrier to adsorption at any of the considered oxygen coverages. However, the conclusion that O adsorption in lb sites on Fe(110) is a barrier-less process holds only for atomic oxygen. The differential heat of adsorption decreases much more than for adsorption on the more open Fe(100) surface. Already at a precoverage of $1/2$ ML the energy gain by adsorbing an additional O atom is only about 3.5 eV, i.e. only slightly larger than the energy required to dissociate an O_2 molecule ($E_{\text{diss}} = 3.15$ eV$/$atom). Under these circumstances, dissociative adsorption of oxygen molecules becomes an activated process.

The different reactivities of the Fe(100) and Fe(110) surfaces is also reflected in the coverage-dependence of the integrated adsorption energy, E_{ad}, calculated from equation (2) (compare figure 2). E_{ad} decreases linearly from the value at a clean surface to less than half the value at full monolayer coverage. The weaker binding is also reflected in the O–surface distance increasing by about 13% with the O-coverage (figure 4), from 1.00 Å at 0.25 ML to 1.15 Å at 1 ML. The coverage dependence of the magnetic moments also shows a quite different behaviour than on the (100) surface. At low O-coverage, the magnetic moment of Fe in the top layer increases from 2.74 μ_B on the clean surface to a maximum value of 3.06 μ_B for $\Theta = 0.5$ ML, dropping abruptly to $\sim$2.7 μ_B on further O-uptake.

At these coverages, the O/Fe(110) surface is already thermodynamically unstable with respect to the formation of FeO. Very recently, the formation of FeO(111) films by exposure of an Fe(110) surface to atomic or molecular oxygen has been investigated by Busch *et al* [19] using Auger electron spectroscopy, low-energy electron diffraction and grazing-incidence ion scattering. It was demonstrated that for oxidation by atomic instead of molecular oxygen the gas exposure required for growing an FeO film can be reduced by almost two orders of magnitude because dissociation and sticking do not limit the growth process. Exposure to atomic oxygen leads to the formation of a well ordered FeO(111) film with a low defect concentration. However, the ion-beam triangulation shows that the formation of a well ordered FeO(111) film is hampered by the mismatch between the rectangular geometry of the Fe(110) surface and the hexagonal geometry of the FeO(111) planes. This agrees with our result that, although atomic oxygen adsorption on O/Fe(110) with $\Theta \geqslant 0.5$ ML remains an unactivated process, a chemical potential of $\mu_O \geqslant -1$ eV is required (see [24]) to stabilize the homogeneous $p(1 \times 1)$ O/Fe(110) adlayer relative to insular growth of FeO.

The formation of thicker iron-oxide film requires the diffusion of oxygen atoms to subsurface positions. It is worth mentioning here that ultraviolet photoelectron spectroscopy measurements [43] suggest that oxygen penetrates into the bulk already at $\Theta > 0.4$ ML. Again this agrees with the observation that the adsorption energies for subsurface O compete with those calculated for dense adlayers [24].

4. Summary

We have presented DFT calculations of the potential-energy profiles for the adsorption of atomic oxygen on the (100) and (100) surfaces partially precovered with oxygen. The variation of the potential energy of the oxygen atom along the bottom of a straight vertical adsorption channel leading to the stable adsorption site (the fourfold hollow on Fe(100) and the long-bridge site on Fe(110)) shows that up to full monolayer coverage the adsorption of atomic oxygen remains a non-activated process. The variation of the *differential* adsorption energy with increasing coverage, however, shows a quite different behaviour on both surfaces. On the more open Fe(100) surface, lateral interactions between the adsorbates are rather weak, and the differential heat of adsorption precovered with 0.75 ML oxygen is only 17% lower than on a clean substrate. On the close-packed Fe(110), strong lateral interactions lead to a pronounced decrease of the differential heat of adsorption with the O-precoverage—already at $\Theta = 0.5$ ML the energy gain on adsorbing an additional O atom is only slightly larger than the energy (per atom) required to dissociate an oxygen molecule.

These differences strongly affect the formation of thin-film oxides. Exposure of a Fe(100) surface to atomic or molecular oxygen leads to the formation of a compact $p(1 \times 1)$ monolayer corresponding to a two-dimensional FeO(100) oxide film. Differences between exposure to atomic and molecular oxygen will appear only close to completion of the O-monolayer and at elevated temperature where the kinetics of the dissociation process becomes important—this, however, goes beyond the scope of the present work. For the Fe(110) surface, only exposure to atomic oxygen can induce the growth of an epitaxial FeO(111) film. Oxidation by exposure to low doses of molecular oxygen is limited to low coverages because of the strong decrease of the differential heat of adsorption. At coverages of 0.5 ML or larger, dissociative adsorption is an activated process. The precise determination of the coverage-dependent dissociation barrier, however, remains a challenge for future study.

Acknowledgments

This work was partly supported by the Polish Ministry of Science in the years 2005–2006 within the Research Project No. 1 P03B 114 28. PB acknowledges the Center for Computational Material Science at the University of Vienna for the Marie-Curie Research Fellowship of the European Commission.

References

[1] Viefhaus H and Grabke H J 1981 *Surf. Sci.* **109** 1
[2] Jansson C and Morgen P 1990 *Surf. Sci.* **223** 84
[3] Maschhoff B L and Armstrong N R 1991 *Langmuir* **7** 693
[4] Miyano T, Sakisaka Y, Komeda T and Onchi M 1986 *Surf. Sci.* **169** 197
[5] Sakisaka Y, Komeda T, Miyano T, Onchi M, Masuda S, Harada Y, Yagi K and Kato H 1985 *Surf. Sci.* **164** 220
[6] Smentkowski V S and Yates J T 1990 *Surf. Sci.* **232** 113
[7] Wight A, Condon N G, Leibsle F M, Worthy G and Hodgson A 1994 *Surf. Sci.* **331–333** 133
[8] Weissenrieder J, Göthelid M, Månsson M, von Schenck H, Tjernberg O and Karlsson U O 2003 *Surf. Sci.* **527** 163
[9] Kim H J and Vescovo E 1998 *Phys. Rev.* B **58** 14047
[10] Vescovo E, Carbone C, Eberhardt W, Rader O, Kachel T and Gudat W 1993 *Phys. Rev.* B **48** 285
[11] Kim H J, Park J H and Vescovo E 2000 *Phys. Rev.* B **61** 15284
[12] Lu J P, Albert M R, Bernasek S L and Dwyer D J 1989 *Surf. Sci.* **215** 348
[13] Horgan A M and King D A 1970 *Surf. Sci.* **23** 259
[14] Brundle C R 1977 *Surf. Sci.* **66** 581
[15] Brundle C R 1978 *IBM J. Res. Dev.* **22** 235
[16] Narkiewicz U and Arabczyk W 1999 *Langmuir* **15** 5790
[17] Arabczyk W, Narkiewicz U, Klucki K and Freidenberg E 1993 *Appl. Surf. Sci.* **72** 45
[18] Waddill G D and Ozturk O 2005 *Surf. Sci.* **575** 35
[19] Busch M, Gruyters M and Winter H 2006 *Surf. Sci.* **600** 2778
[20] Legg K O, Jona F P, Jepsen D W and Marcus P M 1975 *J. Phys. C: Solid State Phys.* **8** L492
[21] Chubb S R and Pickett W E 1987 *Phys. Rev. Lett.* **58** 1248
[22] Ito O, Ohashi K and Kobayashi H 1994 *Surf. Sci.* **317** 203
[23] Eder M, Terakura K and Hafner J 2001 *Phys. Rev.* B **64** 115426
[24] Błoński P, Kiejna A and Hafner J 2005 *Surf. Sci.* **590** 88
[25] Kresse G and Hafner J 1993 *Phys. Rev.* B **47** 558
Kresse G and Hafner J 1994 *Phys. Rev.* B **49** 1425
[26] Perdew J P, Chevary J A, Vosko S H, Jackson K A, Pederson M R, Singh D J and Fiolhais C 1992 *Phys. Rev.* B **46** 6671
[27] Bagno P, Jepsen O and Gunnarsson O 1989 *Phys. Rev.* B **40** 1997
[28] Moroni E G, Kresse G, Hafner J and Furthmüller J 1997 *Phys. Rev.* B **56** 15629
[29] Vanderbilt D 1990 *Phys. Rev.* B **41** 789
[30] Kresse G and Hafner J 1994 *J. Phys.: Condens. Matter* **6** 8245
[31] Monkhorst H J and Pack J D 1976 *Phys. Rev.* B **13** 5188
[32] Methfessel M and Paxton A T 1989 *Phys. Rev.* B **40** 3616
[33] Kohlhaas R, Donner P and Schmitz-Pranghe N 1967 *Z. Angew. Phys.* **23** 245
[34] Błoński P and Kiejna A 2004 *Vacuum* **74** 179
[35] Neugebauer J and Scheffler M 1992 *Phys. Rev.* B **46** 16067
[36] Bengtsson L 1999 *Phys. Rev.* B **59** 12301
[37] Mills G, Jónsson H and Schenter G K 1995 *Surf. Sci.* **324** 305
[38] Carlisle C I, King D A, Bocquet M L, Cerdá J and Sautet P 2000 *Phys. Rev. Lett.* **84** 3899
[39] Gustafsson J, Mikkelsen A, Borg M, Andersen J N, Lundgren E, Klein C, Hofer W, Schmid M, Varga P, Köhler L, Kresse G, Kasper N, Stierle A and Dosch H 2005 *Phys. Rev.* B **71** 115442
[40] Roth W L 1958 *Phys. Rev.* **110** 1333
[41] Simmons G W and Dwyer D J 1975 *Surf. Sci.* **48** 373
[42] Getzlaff M, Bansmann J and Schönhense G 1999 *J. Magn. Magn. Mater.* **192** 458
[43] Pirug G, Broden G and Bonzel H P 1980 *Surf. Sci.* **94** 323